Theor Appl Climatol (2013) 113:329–336
DOI 10.1007/s00704-012-0785-9

ORIGINAL PAPER

Impact of Northwest Pacific anticyclone on the Indian summer monsoon region

J. S. Chowdary · C. Gnanaseelan · Soumi Chakravorty

Received: 1 June 2012 / Accepted: 18 October 2012 / Published online: 13 November 2012
© Springer-Verlag Wien 2012

Abstract Influence of northwest (NW) Pacific anticyclone on the Indian summer monsoon (ISM), particularly over the head Bay of Bengal and monsoon trough region, is investigated. Strong NW Pacific anticyclone during summer induces negative precipitation anomalies over the head Bay of Bengal and Gangetic Plain region. Westward extension of moisture divergence and dry moisture transport from NW Pacific associated with anticyclone (ridge) and local Hadley cell-induced subsidence are responsible for these negative precipitation anomalies. The impact is maximum when the anticyclone and Indian Ocean basin warming co-occur. This contributes significantly to year-to-year variability of ISM.

1 Introduction

Anomalous high-pressure system with an anticyclonic surface circulation over the northwest (NW) Pacific begins to appear in the lower troposphere during the mature phase (winter; seasons are defined like those of the Northern Hemisphere) of El Niño-Southern Oscillation (ENSO; Zhang et al. 1996; Wang et al. 2000). The central Pacific warming helps to set up a favorable large-scale environment for establishment and maintenance of NW Pacific anticyclone through effective air–sea interactions (Wang et al. 2000; Lau and Nath 2003). The central Pacific warming in winter generates the equator-ward flow to the west of the warming, strengthening the mean northeasterlies in the Northern Hemisphere, which in turn intensify the evaporative cooling in the NW Pacific (Wang et al. 2000). The sea surface temperature (SST) cooling generates an anticyclone to the west due to a Rossby wave response of suppressed convective heating (Wang et al. 2000). NW Pacific anticyclone (wind anomalies) and surface high during winter and spring are originated and maintained by the positive thermodynamic feedback with in situ negative SST anomalies, suggestive of a local ocean–atmosphere interaction (Wang et al. 2000; Lau and Nath 2003). However, such a local feedback is not applicable for the persistence of summer anticyclone as there is very weak (or negative) correlation between local SST and rainfall. During summer, the NW Pacific anticyclone is instead induced remotely by the tropical Indian Ocean (TIO) SST (Xie et al. 2009) and is strongly correlated with the preceding El Niño (Wang et al. 2000; Xie et al. 2009).

The tropical Pacific exerts strong influence over TIO SST variability during the mature phase of El Niño via teleconnections (Klein et al. 1999; Alexander et al. 2002; Xie et al. 2009). El Niño-induced basin-wide TIO warming persists from winter to next summer and substantially impacts the NW Pacific climate (Xie et al. 2009). The persistent TIO warming influences the atmospheric circulation over south Asia during summer following El Niño (Yang et al. 2007).

The westward extension of the NW Pacific anticyclone mainly drives the summer rainfall variability in East Asia (Wang et al. 2000) and the convection over the western Pacific region. Moisture supply by the southwesterlies on the northwest flank of the anticyclone leads to enhanced precipitation over the northeast China and Japan (Wang et al. 2000; Chowdary et al. 2011). Stronger convection over the western Pacific warm-pool region is associated with the eastern flank of NW Pacific anticyclone (Lu and Dong 2001). Though the influence of NW Pacific anticyclone on

J. S. Chowdary (✉) · C. Gnanaseelan · S. Chakravorty
Indian Institute of Tropical Meteorology,
411008, Pune, Maharastra, India
e-mail: jasti@tropmet.res.in

the East-Asian summer monsoon is well established, its impact on the rainfall over the Indian summer monsoon (ISM) region is not systematically studied in the past. The present study addresses this issue in detail, focusing mainly on the rainfall variability over the head Bay of Bengal and monsoon trough region.

The paper is organized as follows. The following section outlines the details of different data sets used in the study. Section 3 presents the dominant mode of variability in the NW Pacific mean sea level pressure (SLP). Section 4 discusses the influence of NW Pacific anticyclone on the ISM. Underlying mechanisms responsible for rainfall anomalies (in the ISM region) associated with NW Pacific anticyclone is discussed in Section 5. The summary is provided in Section 6.

2 Data used

The Center for Climate Prediction merged analysis for precipitation (Xie and Arkin 1997) and the European Centre for Medium-Range Weather Forecasts reanalysis Interim (ERA-Interim; Dee et al. 2011) data are utilized in the study. ERA-Interim is the recent global atmospheric reanalysis covering the period from 1979 to the present and has a horizontal resolution of 1.5° longitude×1.5° latitude with 37 pressure levels vertically. Monthly means of selected variables such as SLP, surface winds, three-dimensional specific humidity and winds are obtained from ERA-Interim reanalysis. The National Oceanic and Atmospheric Administration/National Climate data Center Extended Reconstruction SST version 2 (Smith and Reynolds 2004) is used for the ocean analysis. High-resolution gridded monthly land rainfall data over the Indian subcontinent is obtained from the Indian Meteorological Department (1,803 stations) for the period of 1979–2010 (Rajeevan et al. 2006). Various statistical techniques such as empirical orthogonal function (EOF), correlation and regression are carried out in the present study. In addition to these, vertically integrated moisture divergence and transport are computed to determine the associated physical mechanisms. Niño3.4 (TIO SST) index is calculated as the average SST anomalies over 170°W–120°W, 5°S–5°N (40°E–100°E, 20°S–20°N). To remove the effect of pronounced intra-seasonal variability over the Indo-western Pacific Ocean, a 3-month running average is applied for all data over the study period of 1979–2010.

3 Dominant mode of NW Pacific SLP

Figure 1a shows the spatial pattern of summer (JJA; Jun–July–August) NW Pacific SLP EOF-1, which exhibits NW Pacific high extending East-Asian land mass with the largest loading around 20°N and 150°E (Xie et al. 2009; Chowdary et al. 2011). The anomalous anticyclone is consistent with the rainfall distribution over the NW Pacific and suggestive of their local feedback (Chowdary et al. 2010). Not only local precipitation but also rainfall over the Indian subcontinent (mainly over the monsoon trough region) is influenced by the NW Pacific anticyclone. The correlation pattern of land rainfall over the Indian subcontinent with the first principal component (PC-1, hereafter PC; Fig. 1c) of SLP is displayed in Fig. 1b. The correlation of 0.30 is significant at 90 % confidence level for 32 years based on two-tailed student *t* test. The NW Pacific JJA SLP PC-1 shows positive peaks during 1979, 1980, 1983, 1988, 1992, 1996, 1998, 1999, 2003, 2008, and 2010. Selection of NW Pacific anticyclone is based on PC being more than half standard deviation. About 50 % of the above years are following El Niño events (summers), which strongly support the role of El Niño in maintaining the summer anticyclonic circulation. The temporal correlation of PC is 0.40 when correlated (lagged) with NDJ(0/1) [November(0)–December(0)–January(1)] Niño 3.4, which is significant at 95 % confidence level. Therefore, it is essential to examine the impact of NW Pacific anticyclone on the ISM rainfall when anticyclone is associated with El Niño (or with TIO warming) and the years when anticyclone is not associated with El Niño/TIO warming. In this paper, we denote seasons during the developing and decay years of El Niño with (0) and (1), respectively.

The TIO basin-wide warming increases the tropospheric temperature via deep convection, emanating a baroclinic Kelvin wave into the equatorial Pacific (Xie et al. 2009). The warm Kelvin wave wedge lowers the SLP in the equatorial western Pacific, inducing northeasterly surface wind anomalies over the subtropical NW Pacific (Xie et al. 2009; Chowdary et al. 2011). The resultant divergence in the subtropical NW Pacific suppresses convection. Strong TIO warming associated with El Niño translates into a pronounced development of atmospheric anomalies over the NW Pacific (Xie et al. 2009) and South Asia (Yang et al. 2007) during JJA(1) though direct influence of El Niño fade away. This shows that El Niño does have strong influence on the NW Pacific anticyclone in JJA(1) through the warm TIO SST anomalies. NW Pacific anticyclone strength is high in most of the summer following El Niño compared to other years.

4 Influence of NW Pacific anticyclone on ISM rainfall

The NW Pacific anticyclone affects summer climate in most of the Indo-western Pacific region. Figure 2a–c

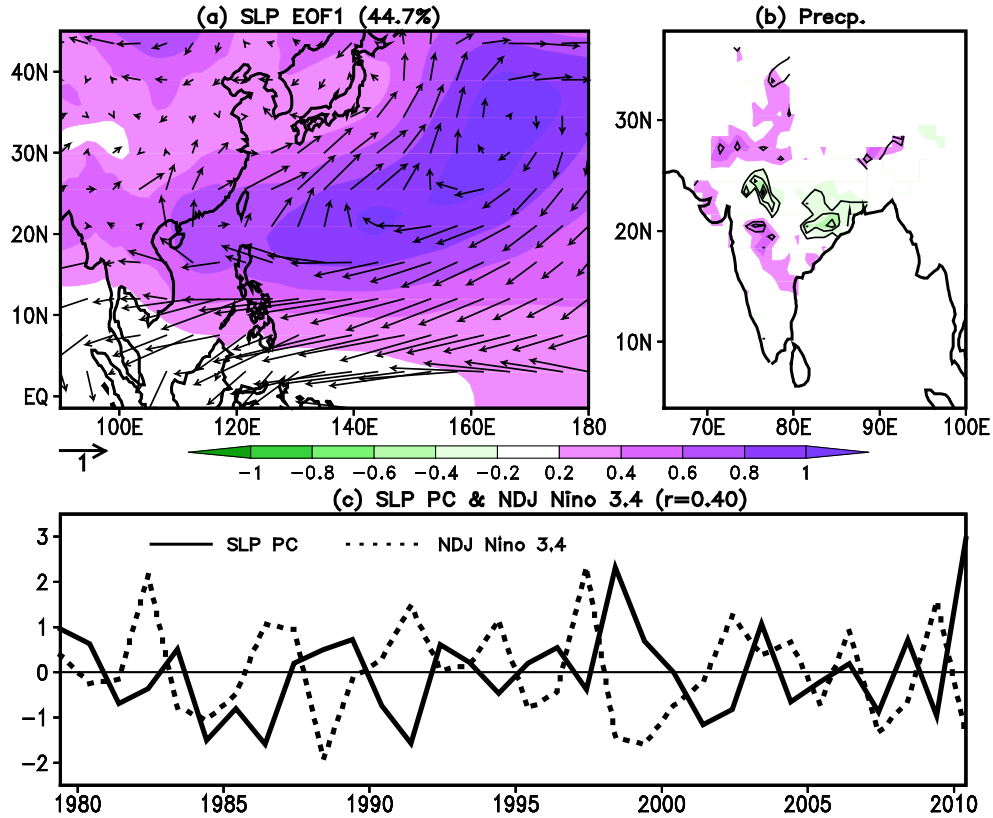

Fig. 1 **a** The first EOF of JJA SLP anomalies (hPa; shaded) and 850 hPa wind anomalies (in meters per second; *vectors*) regressed against the corresponding SLP principal component (PC), **b** NW Pacific SLP PC correlation with JJA rainfall (only over Indian land mass), and **c** NW Pacific SLP PC and NDJ(0/) Niño 3.4 time series

show correlation of summer precipitation and 850 hPa winds with the JJA SLP PC, NDJ(0/1) Niño 3.4 and JJA TIO SST indices, respectively. Correlation with NW Pacific SLP PC shows enhanced precipitation anomalies over the maritime continent, west of India, and from East China to Japan and decrease over the Gangetic Plain and NW Pacific regions (Fig. 2a). Strong negative precipitation over the southwest TIO and intensified-cross equatorial flow are also evident in Fig. 2a. Over the north Indian Ocean, northeasterly wind anomalies, associated with the anticyclone are mainly responsible for the sustained local warming (Fig. 2d; Du et al. 2009; Chakravorty et al. 2012). Correlation with NW Pacific SLP PC shows that most of the TIO and some parts of the western Pacific Ocean are covered with positive SST anomalies. SLP high in the NW Pacific extend up to the head Bay of Bengal driving suppressed convection (Fig. 2d).

Negative rainfall over the NW Pacific and positive over the TIO and the maritime continent are apparent when correlated with NDJ(0/1) Niño3.4 (Fig. 2b). The NW Pacific 850 hPa wind correlation closely resembles the regression of SLP PC (Fig. 1a) which is characterized by anticyclonic circulation. TIO warming during JJA(1) is a robust feature when correlated with NDJ(0/1) Niño 3.4 (Fig. 2e). NW Pacific anticyclone center is shifted to west of its normal position due to the El Niño forcing. Anomalous anticyclonic wind associated with high pressure over the NW Pacific is seen when correlated with JJA TIO SST index (Fig. 2c). It is important to note that SST correlation with TIO SST index displays different spatial pattern compared to other two indices. Strong positive correlation is seen over the western and central TIO, whereas weak correlation prevails in the southeastern TIO. This suggests that the JJA cooling signals in the southeastern TIO during the Indian Ocean Dipole (Saji et al. 1999) years compensate the interannual warming thereby weakening the correlation there (Fig. 2f). SLP displays similar spatial patterns over the Indo-western Pacific when correlated with NW Pacific SLP PC and TIO SST index (Fig. 2f). For further analysis, we have used correlation with NW Pacific SLP PC and NDJ (0/1) Niño 3.4 (lagged) indices. The analysis reveals that rainfall is weak over the head Bay of Bengal and Gangetic Plain regions and strong over the west coast of India when correlated with NDJ(0/1) Niño 3.4/NW Pacific SLP PC during summer. To verify the impact of decadal or long-term variations in this interannual signals, we have removed the 9-year running mean from dataset and no significant changes are noticed (figure not shown). This indicates that longer variations such as decadal changes have very less impact on the current results. Especially, signals over the NW Pacific and north Indian Ocean regions showed similar patterns.

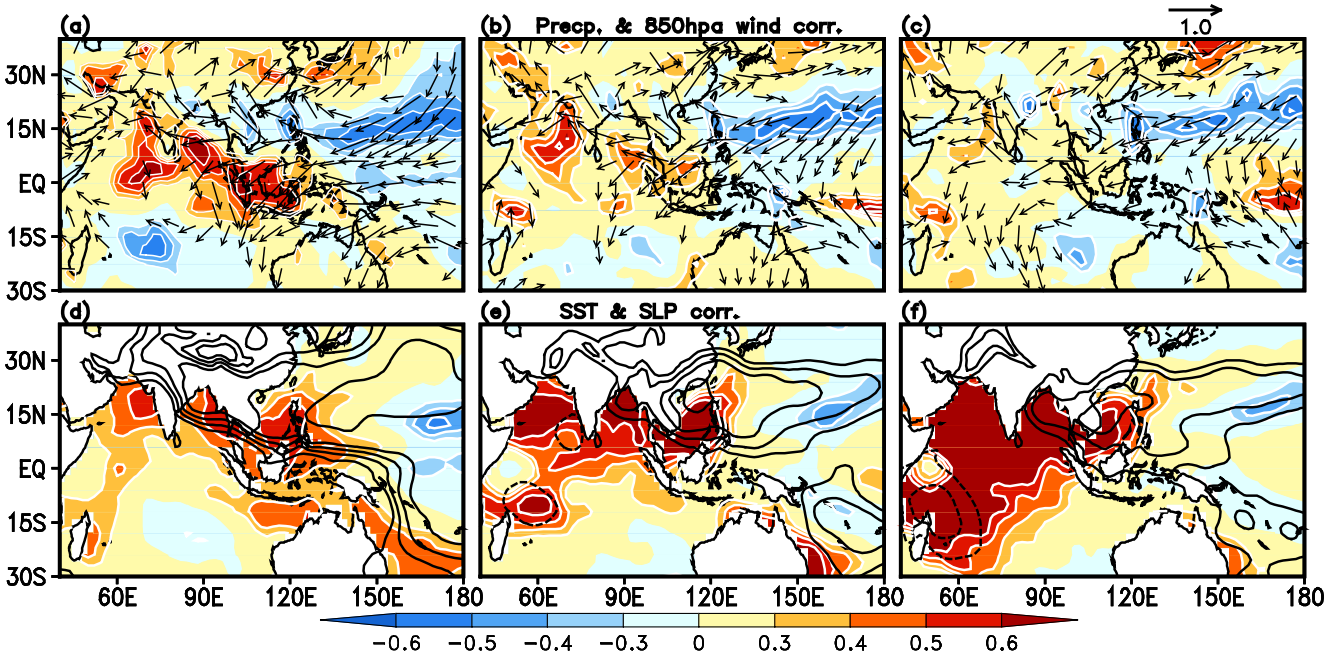

Fig. 2 **a** Correlation of JJA precipitation (*shaded*) and 850 hPa winds (*vectors*) with NW Pacific SLP PC, **b** same as **a** but correlation with NDJ(0/1) Niño-3.4 SST (lagged) and **c** same as **a** but correlation with JJA TIO SST index. **d**–**f** same as **a**–**c** but for SST (*shaded and white contours*) and SLP (*black contours*). Contours represent correlation above 0.3

5 Possible mechanisms

A partial correlation analysis was performed between NW Pacific SLP PC and rainfall (850 hPa wind) anomalies over the Indo-western Pacific after removing the effect of the preceding El Niño (Fig. 3a). In response to SLP high, anticyclonic circulation is strong over the NW Pacific and extend to head Bay of Bengal and some parts of Indian subcontinent (correlation is weak). A ridge extension causes the head Bay of Bengal and Gangetic Plain region to dry. Negative rainfall correlation is apparent over the southwest TIO (south of 10°S). In contrast, positive rainfall band in response to NW Pacific high is seen over the equatorial TIO including maritime continent. SLP spatial pattern is consistent with rainfall distribution over the NW Pacific and north Indian Ocean (Fig. 3b). SST is warm only in some parts of the north Indian Ocean and negative over the south-central TIO (Fig. 3b). SST correlations in the equatorial Indian Ocean are weak in response to NW Pacific high. Strong moisture divergence associated with anomalous anticyclone is responsible for negative rainfall anomalies over the NW Pacific (Fig. 3c). Vertically integrated moisture divergence extended towards head Bay of Bengal in association with anticyclone and induced low rainfall in Gangetic plain region (Fig. 3c). Moisture divergence and transport support the distribution of rainfall pattern especially over the southwest TIO and maritime continent.

Partial correlations with NDJ(0/1) Niño 3.4 SST by removing NW Pacific high influence is shown in Fig. 3d. Rainfall correlation is positive over the maritime continent, eastern Arabian Sea and southwest TIO. Negative rainfall correlations are seen over the NW Pacific and some parts of monsoon trough region. Wind pattern over the north Indian Ocean is similar to their correlation with NW Pacific SLP PC. Figure 3d shows evidence of anomalous summer anticyclone over the NW Pacific in response to preceding El Niño. Over the western TIO, wind anomalies are northeasterlies to north and northwesterlies to the south of the equator when correlated (partial) with NDJ(0/1) Niño 3.4 index. These wind anomalies are against the mean winds, causing warm SST in this region by reducing evaporation (Du et al. 2009). TIO is warmer in response to El Niño during JJA(1). Strong moisture convergence and warm SST are responsible for enhanced rainfall over the western TIO (Fig. 3d and f). The weak low-level winds do not necessarily represent the monsoonal convective strength (Park et al. 2010). Moist processes such as moist stability and moisture transport associated with the warmer north Indian Ocean compensate for the wind effect (Yang et al. 2007; Park et al. 2010). Thus, enhanced rainfall over Western Ghats and Southern peninsular India in JJA(1) is due to the El Niño-induced TIO warming. Increased rainfall over maritime continent is also associated with local SST and moisture convergence (Fig. 3f). On the

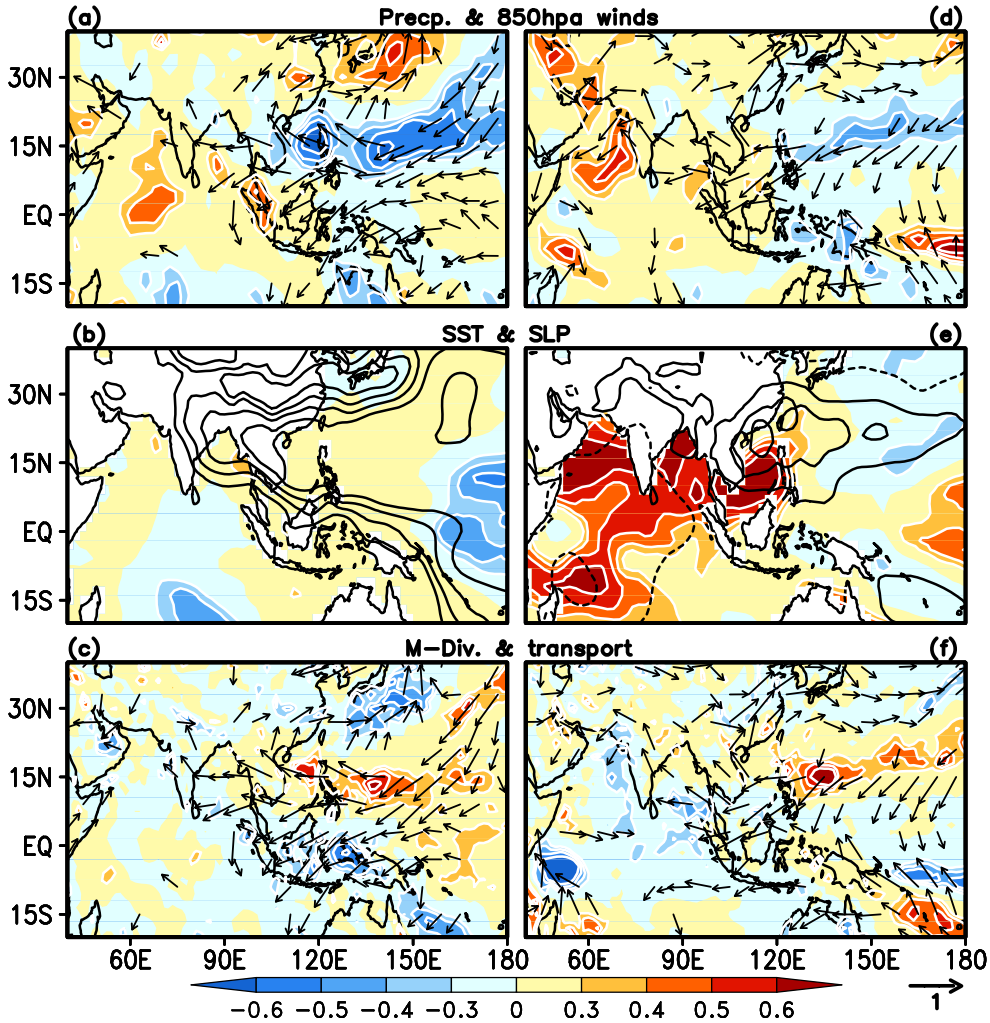

Fig. 3 Partial correlation of NW Pacific JJA SLP PC (effect of the preceding El Niño (NDJ (0/1) Niño-3.4) is removed) with anomalies of **a** precipitation (*shaded*) and 850 hPa (*vectors*), **b** SST (*shaded*) and SLP (*contour*), and **c** vertically integrated moisture divergence (*shaded*) and transport (*vectors*). **d**–**f** same as **a**–**c** but correlation (lagged) with NDJ(0/1) Niño-3.4 SST index (NW Pacific anticyclone (JJA SLP PC) influence is removed)

other hand, strong moisture divergence associated with anomalous anticyclone over the NW Pacific is responsible for negative rainfall anomalies in this region. Moisture divergence extended towards head Bay of Bengal suppresses rainfall over the monsoon trough region. In general, the moisture transport from adjacent seas exerts important influences on ISM rainfall. Figure 3c and f show that wind (transport) anomalies associated with anomalous westward (northwestwards) extension of NW Pacific anticyclone are opposite to the climatological forcing. This helps to reduce the mean moisture transport over the monsoon trough and head Bay of Bengal regions. The weak mean moisture transport thereby accounts for the decreased rainfall over the central and northeast India. The circulation responsible for dry moisture transport into the continent is associated with NW Pacific anticyclone.

Figure 4a illustrates climatological JJA Hadley cell (averaged zonally between 80°E and 100°E) with upward motions from 10°S to 25°N and subsidence in the region south of 10°S. During the years of strong anticyclone, weakening of upward motion over the head Bay of Bengal (including some parts of Indian land region) and strengthening over the equatorial region are evident (Fig. 4b and c). This shows the weakening of large-scale monsoon Hadley cell. Partial correlation revealed that strong divergence over NW Pacific causes anomalous convergence over the maritime continent (which is a positive feedback) and southern Bay of Bengal (Fig. 3c). Enhanced convection over this region produces upward motion and resultant subsidence is seen in the region north of 15°N (Fig. 4b). This further reduces the rainfall over head Bay of Bengal and some parts of northeast India. Anomalous divergence supports this claim. Similar circulation pattern is evident when correlated with NDJ(0/1) Niño 3.4 (lagged). Convection over the east equatorial Indian Ocean is associated with local warm SST and NW Pacific high (Fig. 3d and e). Upward motion in the region south of 10°N and subsidence in the north are apparent in Fig. 4c. Anomalous Hadley cells in both cases provide dynamical support for subsidence over the head Bay of Bengal and enhanced convection in the east equatorial Indian Ocean.

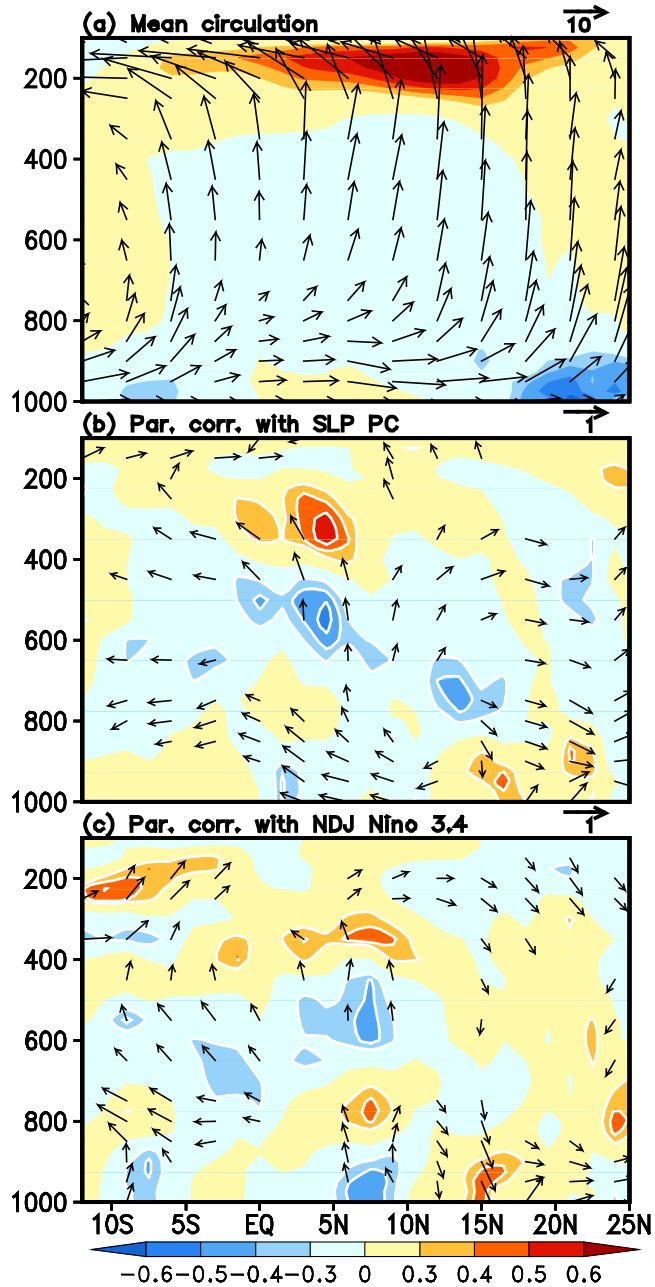

Fig. 4 **a** The JJA climatological horizontal divergence (in per second) at different levels (*shaded*) and monsoon Hadley cell shown by the cross-section of meridional and vertical wind components (*vectors*) averaged longitudinally between 80–100°E. The vertical velocity (10^{-2} Pa s^{-1}) is taken with *negative sign*. **b** Same as in **a** except for partial correlation with NW Pacific JJA SLP PC (effect of the preceding El Niño (NDJ(0/1)) Niño-3.4) and **c** same as **a** except for partial correlation NDJ(0/1) Niño-3.4 SST index (NW Pacific anticyclone (JJA SLP PC) influence is removed)

Overall, extended moisture divergence from NW Pacific (associated with anticyclone) and local Hadley cell-induced subsidence are responsible for negative precipitation anomalies over the head Bay of Bengal and monsoon trough region. It is important to note that both NW Pacific anticyclone and warm TIO SST anomalies together produce strong impact on ISM rainfall than the individual forcing. This is supported by the total correlation of SLP PC with moisture divergence and local Hadley cell (Fig. 5). Correlation of NDJ Niño 3.4 also displayed similar strong moisture divergence and subsidence in the region north 10°N (figure not shown).

6 Summary

We examined the impact of JJA NW Pacific anticyclone on the ISM, in particular, over the head Bay of Bengal and monsoon trough regions. Anomalous NW Pacific anticyclone is known to occur during summer after peak phase of El Niño, which is strongly influenced by El Niño-induced TIO SST warming (Xie et al. 2009). Local air–sea interactions and central Pacific cooling are important for maintaining the anticyclone when it is not associated with El Niño/TIO warming (Chowdary et al. 2010). It is observed that 50 % of summer NW Pacific anticyclone years are independent of El Niño and TIO warming. Therefore, impact of NW

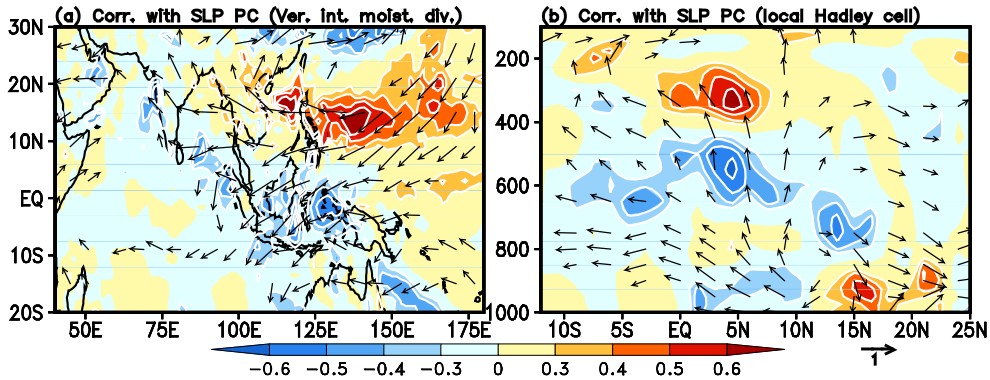

Fig. 5 Correlation of the NW Pacific JJA SLP PC with anomalies of **a** vertically integrated moisture divergence (*shaded*) and transport (*vectors*) and **b** horizontal divergences (*shaded*) and meridional and vertical wind components (*vectors*) averaged longitudinally between 80 and 100°E (monsoon Hadley cell). The vertical velocity is taken with *negative sign*

Pacific anticyclone on ISM is investigated using partial correlation analysis to isolate the individual forcing.

We found that NW Pacific anticyclone co-occurring with TIO basin-wide warming produce strong impact on ISM. Two possible mechanisms are identified. One is westward extension of moisture divergence from NW Pacific associated with anticyclone (ridge) and second is the subsidence related to local Hadley cell. Both mechanisms together are primarily responsible for negative precipitation anomalies over the head Bay of Bengal and monsoon trough region. Strong convection over the east equatorial Indian Ocean and maritime continent causes subsidence in the region north of 15°N through local Hadley cell, providing dynamical support.

The summer NW SLP PC is highly correlated (r=0.57) with JJA ISM rainfall PC-4 (Fig. 6; corresponding to EOF-4). The fourth leading mode of the JJA ISM rainfall accounts for 6.54 % variability which involves a pattern of precipitation with negative sign in the Gangetic Plain region and above normal rainfall over peninsular India to the east of the Western Ghats. Higher modes of ISM rainfall and their relationship with SST and circulation are examined by Mishra et al. (2012). It is important to note that the variance explained by EOF-2 in their study is 9 %. Thus, it is essential to understand atmospheric patterns related to ISM rainfall interannual variability though percentage of variance explained by EOF modes is relatively less. Spatial patterns of SLP (correlation) and circulation (regression

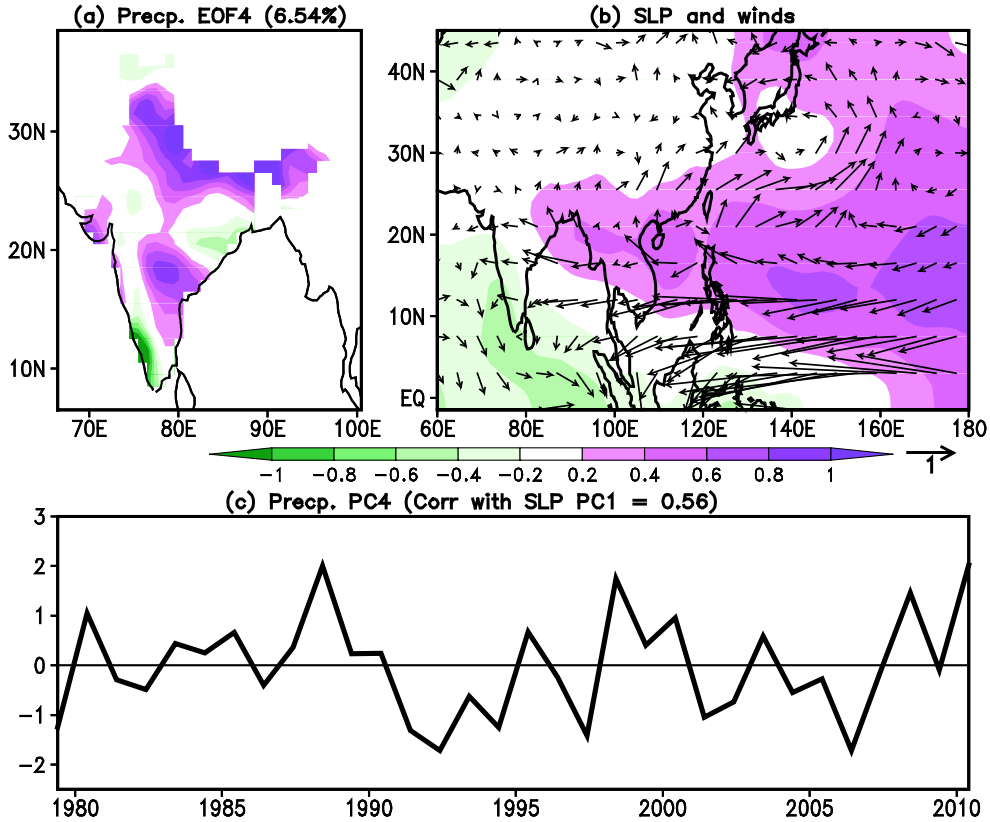

Fig. 6 **a** JJA precipitation EOF-4 (in millimeters per day) for Indian land mass, **b** correlation of SLP and regression of 850 hPa wind anomalies (in meters per second) with rainfall PC corresponding to (**a**), and (**c**) rainfall PC time series

with PC-4) corresponding to ISM rainfall EOF-4 is shown in Fig. 6b. These patterns are similar to NW Pacific anticyclone (Fig. 1a), indicating the importance of its contribution to interannual variability of ISM rainfall through moisture divergence and local Hadley cell.

Acknowledgments We thank Prof. B. N Goswami Director IITM for support. We are grateful to Prof. Shang-Ping Xie and Prof. Bin Wang (IPRC) for discussion. We thank anonymous reviewers for their valuable comments that helped us to improve the manuscript. Figures are prepared in GrADS.

References

Alexander MA, Bladé I, Newman M, Lanzante JR, Lau NC, Scott JD (2002) The atmospheric bridge: the influence of ENSO teleconnections on air–sea interaction over the global oceans. J Climate 15:2205–2231

Chakravorty S, Chowdary JS, Gnanaseelan C (2012) Spring asymmetric mode in the tropical Indian Ocean: Role of El Niño and IOD. Clim Dyn. doi:10.1007/s00382-012-1340-1

Chowdary JS, Xie SP, Lee JY, Kosaka Y, Wang B (2010) Predictability of summer Northwest Pacific climate in eleven coupled model hindcasts: local and remote forcing. J Geophys Res 115:D22121. doi:10.1029/2010JD014595

Chowdary JS, Xie SP, Luo JJ, Hafner J, Behera S, Masumoto Y, Yamagata T (2011) Predictability of Northwest Pacific climate during summer and the role of the tropical Indian Ocean. Clim Dyn 36:607–621. doi:10.1007/s00382-009-0686-5

Dee DP et al (2011) The ERA-Interim reanalysis: configuration and performance of the data assimilation system. Q J Roy Met Soc 137:553–597

Du Y, Xie SP, Huang G, Hu KM (2009) Role of air–sea interaction in the long persistence of El Niño-induced North Indian Ocean warming. J Climate 22:2023–2038

Klein SA, Soden BJ, Lau NC (1999) Remote sea surface temperature variations during ENSO: evidence for a tropical atmospheric bridge. J Climate 12:917–932

Lau NC, Nath MJ (2003) Atmosphere–ocean variations in the Indo-Pacific sector during ENSO episodes. J Climate 16:3–20

Lu R, Dong BW (2001) Westward extension of North Pacific subtropical high in summer. J Met Soc Japan 79:1229–1241

Mishra V, Smoliak BV, Lettenmaier DP, Wallace JM (2012) A prominent pattern of year-to-year variability in Indian Summer Monsoon Rainfall. PNAS. doi:10.1073/pnas.1119150109

Park HS, Chiang JCH, Lintner BR, Zhang GJ (2010) The delayed effect of major El Niño events on Indian monsoon rainfall. J Climate 23:932–946

Rajeevan M, Bhate J, Kale JD, Lal B (2006) A high-resolution daily gridded rainfall for the Indian region: analysis of break and active monsoon spells. Curr Sci 91:296–306

Saji NH, Goswami BN, Vinayachandran PN, Yamagata T (1999) A dipole mode in the tropical Indian ocean. Nature 401:360–363

Smith TM, Reynolds RW (2004) Improved extended reconstruction of SST (1854–1997). J Climate 17:2466–2477

Wang B, Wu R, Fu X (2000) Pacific-East Asian teleconnection: how does ENSO affect east Asian climate? J Climate 13:1517–1536

Xie P, Arkin PA (1997) Global precipitation: a 17-year monthly analysis based on gauge observations, satellite estimates, and numerical model outputs. Bull Am Meteorol Soc 78:2539–2558

Xie SP, Hu K, Hafner J, Tokinaga H, Du Y, Huang G, Sampe T (2009) Indian Ocean capacitor effect on Indo-western Pacific climate during the summer following El Niño. J Climate 22:730–747

Yang J, Liu Q, Xie SP, Liu Z, Wu L (2007) Impact of the Indian Ocean SST basin mode on the Asian summer monsoon. J Geophys Res 34:L02708. doi:10.1029/2006GL028571

Zhang R, Sumi A, Kimoto M (1996) Impacts of El Niño on the East Asian monsoon: a diagnostic study of the '86/87 and '91/92 events. J Met Soc Japan 74:49–62